# Temperature distribution and heat losses in molten salts tanks for CSP plants

Cristina Prieto[1], Laia Miró[2], Gerard Peiró[2], Eduard Oró[2,*], Antoni Gil[2,**], Luisa F. Cabeza[2,†]

[1]Abengoa Research. C/Energía Solar 1,41012, Seville, Spain.

[2] GREA Innovació Concurrent, Universitat de Lleida, Edifici CREA, Pere de Cabrera s/n, 25001, Lleida.

*Present address: IREC, Jardins de les Dones de Negre 1, 2ª pl.08930 Sant Adrià de Besòs Barcelona, (Spain)

**Present address: Department of Mechanical Engineering, Massachusetts Institute of Technology, 77 Massachusetts Avenue, Cambridge, MA 02139, United States of America

[†]Corresponding author: Tel.: +34.973.00.35.76. email: lcabeza@diei.udl.cat

**Abstract**

Solar power plants have been deployed in the last 20 years, so the interest in evaluating their performance is growing more and more. In these facilities, thermal energy storage is used to increase dispatchability of power. The two-tank molten salts storage system with "solar salt" (60 wt.% $NaNO_3$ and 40 wt.% $KNO_3$) is the one commercially used today. To be able to achieve a deep understanding of the two-tank solar storage systems with molten salts, in 2008 a pilot plant was built at the University of Lleida (Spain) and the experimental evaluation of the temperature distribution inside the tanks and their heat losses are presented in this paper. Therefore, this pilot plant is equipped with several temperature sensors inside the tank as well as in the different layers of external insulation. As expected, temperature is lower at the external part of the tank (near the cover, at the bottom and near the walls) and no stratification is seen. It is found that the influencing parameters in the temperature distribution of the salts inside the tank are: insulation, and the existence of different electrical resistances and the orientation and surroundings of the tank. Heat losses were measured and compared both with a simulated 1-D steady state model and previous literature. Measured heat losses were from 61 $W/m^2$ through the bottom to 80 $W/m^2$ through the walls (with 73 $W/m^2$ through the cover).

**Keywords:** Storage; Temperature distribution; High temperature; Molten salts; Two-tanks; Heat losses

**Nomenclature**

| | |
|---|---|
| $A_{Concrete}$ | Heat transfer area of concrete [$m^2$] |
| $A_{cyl}$ | Heat transfer area of tank walls [$m^2$] |
| $A_{sphere}$ | Heat transfer area of top tank wall [$m^2$] |
| Cp | Specific heat of salts [J/kg·ºC] |
| h | Convection heat transfer coefficient between tanks and ambient [$W/m^2$·ºC] |
| $k_{concrete}$ | Thermal conductivity of refractory concrete [W/m·ºC] |
| $k_{Rockwool}$ | Thermal conductivity of Rockwool [W/m·ºC] |
| L | Height of the tank wall [m] |
| $Q_{Concrete}$ | Heat losses through concrete base [W] |
| $Q_{FG}$ | Heat losses through Foamglass base [W] |
| $Q_{Top}$ | Heat losses through the top of the tank [W] |
| $Q_{Wall}$ | Heat losses through the wall of the tank [W] |
| $r_1$ | Outer radius of the tank [m] |
| $r_2$ | Radius of the tank with Rockwool [m] |
| T | Temperature [ºC] |
| $T_{Bottom}$ | Temperature of the bottom of the tank [ºC] |
| $T_{Ground}$ | Temperature of the ground [ºC] |
| $T_{salt}$ | Temperature of the salt in the hot and in the cold tank [ºC] |
| $T_{Wall.ext}$ | Temperature of the Rockwool surface wall of the tank [ºC] |
| $T_{Wall.in}$ | Temperature of the external wall surface of the tank [ºC] |
| V | Volume of storage tanks [$m^3$] |
| $\Delta_{X.Concrete}$ | Thickness of concrete base [m] |
| ρ | Density of salts [$kg/m^3$] |
| ΔT | Thermal gradient between wall of storage tanks and sorrounding air [ºC] |

# 1. Introduction

Sustainable and low-carbon energy technologies will play a crucial role in the energy revolution to change current trends in energy supply and use. Generation of solar thermal electricity from concentrating solar power (CSP) plants has grown strongly worldwide. In fact, CSP components and systems are coming to commercial maturity, holding the promise of increased efficiency, declining costs and higher value through increased dispatchability (International Energy Agency 2014). Four main elements are required in these plants: concentrator, receiver, transport/storage system, and power conversion block (Gil et al. 2010, Medrano et al. 2010). Among them, thermal energy storage (TES) is recognised as the technology that increases the energy system reliability, increases the generation capacity, and reduces the cost of generation. Moreover, TES

has always been associated to solar installations because of the limitation in solar availability, which does not coincide with the energy demand periods.

Several commercial solar power plants exist today (Collado and Guallar 2013, Medrano et al. 2010). Among the different TES systems, two-tanks molten salts is the most used system. A typical scheme of such a system can be seen in Fig. 1. In this configuration, HTF from the solar field is diverted through a heat exchanger that is used to charge the thermal storage system, heating salt from the cold salt tank and storing it in the hot salt tank. When the storage system is discharged, salt from the hot salt tank is sent back to the HTF-salt heat exchanger and is used to heat HTF. The heated HTF is then sent to the power block (Gabrielli and Zamparelli 2009). The main characteristic of two-tank configurations is that the cold and hot TES media (at respectively 298 ºC and 388 ºC, approximately) are stored separately and the system installation and operation is currently very well known by commercial electric power companies.

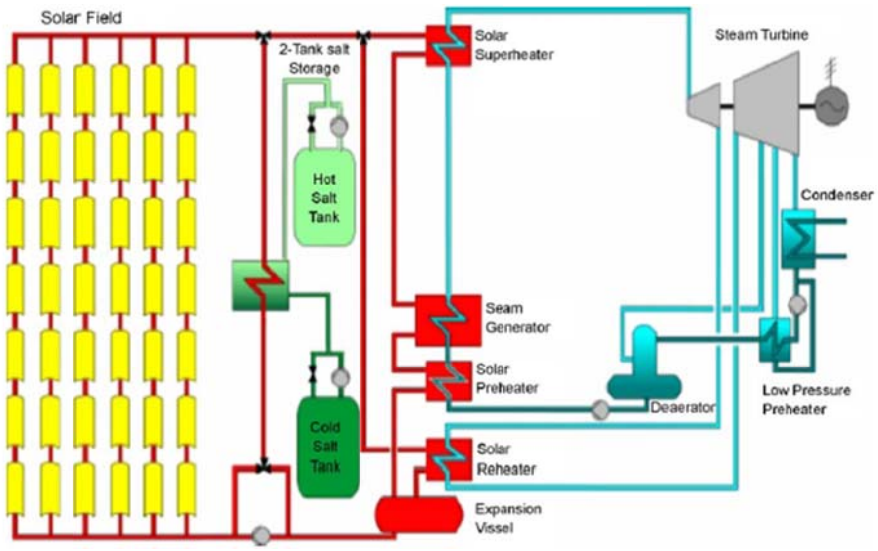


Fig. 1. Scheme of a typical two tanks storage tanks storage system in CSP (Gil et al. 2010).

Different materials have been investigated as thermal storage fluids for parabolic trough solar power plants, but due to economic and safety reasons, the so called "molten salts" or "solar salt" (60% $NaNO_3$ and 40% $KNO_3$) is the one used today (Gabrielli and Zamparelli 2009, Gil et al. 2010 and Moens et al. 2003 ). As Grabrielli and Zamparelli (2009) stated, in a two-tank configuration of a parabolic trough solar power plant with sensible heat thermal storage, the storage tanks are amongst the most critical components. However, no deep studies of the performance of such storage tanks have been published up to now.

To be able to achieve a deep understanding of the two-tank solar storage systems with molten salts, in 2008 a pilot plant was built at the University of Lleida, Spain (Fig. 2). Such pilot plant

allows the study of this molten salts storage tanks system performance while a secondary circuit incorporating thermal oil (Therminol VP1) simulates the solar energy input by the use of a 24 kWe electrical boiler

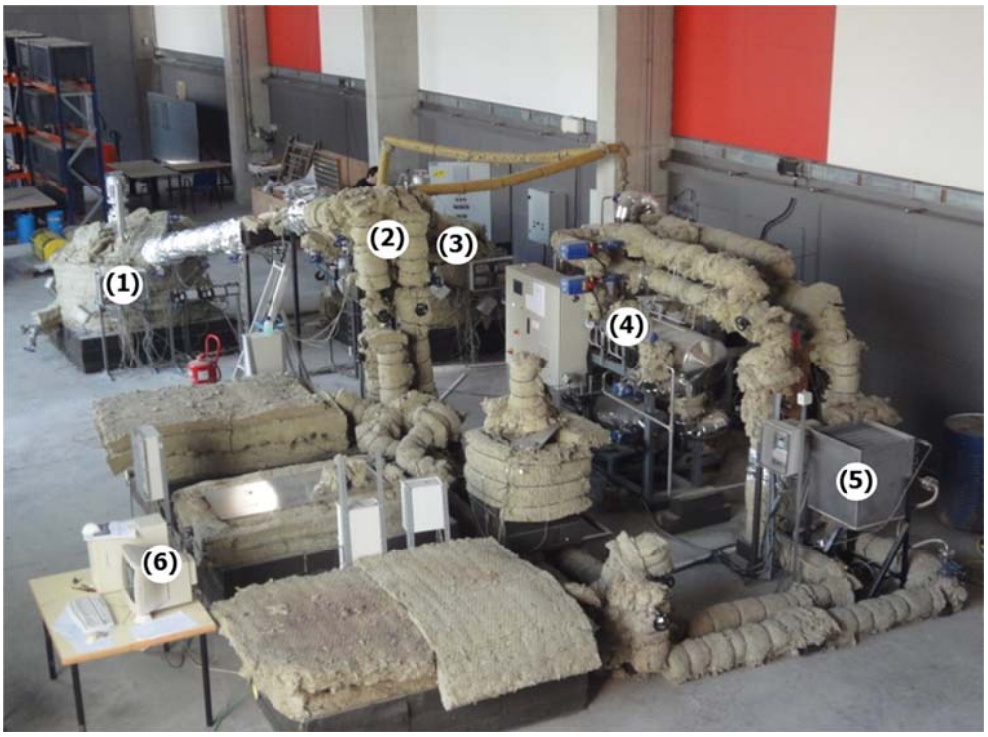


Fig. 2. High temperature pilot plant at University of Lleida, Spain. (1) Hot tank, (2) HTF-salts heat exchanger, (3) Cold tank, (4) Electrical boiler, (5) HTF-air heat exchanger, and (6) acquisition and recording system

Since the two-tanks molten salts system configuration relays on the separation of the hot and cold fluid in two different tanks, its efficiency is based on a constant outlet salt temperature when discharging, which leads to the requirement of no stratification effect in the storage tanks. Therefore, heat losses to the surroundings may represent an important factor on the TES media stratification. In this paper, to evaluate the thermal performance of this two-tanks molten salts system, both the molten salts temperature distribution and the conduction heat losses through the walls of the storage tanks are widely evaluated and discussed taking advantage of the fact that this experimental pilot plant is equipped with many temperature sensors and recording equipment which allows a detailed study that is not possible in other case studies.

There are scarce published papers on experimental heat losses in molten salts reported previously. Pacheco et al. (2002) and Pacheco et al. (1999) reported measured thermal losses in the hot and cold tank in the two-tank Solar Two facility by means of turning off heat tracing and immersion heaters over several days. They accounted for 102 kW and 44 kW in the hot and cold

tank, respectively. Based on the same facility, Hermann et al. (2004) performed a regression analysis to develop an empirical heat loss equation from the measured values. Suarez et al. (2015) calculated numerically the heat losses of the tank depending on the volume of salts inside the tank and compare it with similar numerical studies performed by Zaversky et al. 2013, Rodriguez et al. 2013 and Schulte-Fischedic et al. 2008. Those simulations reveal a very homogeneous temperature distribution in the tank where the minimum temperatures are reached near the tank surfaces, especially near the free surface and the bottom. Thus, similar results are expected in the experimental analysis presented in this study. Moreover, the heat losses are validated both with a mathematical model using EES and with a correlation published by Herrmann et al. 2004.

# 2. Materials and method

## 2.1. Materials

The storage material used in this analysis is a mixture of sodium nitrate and potassium nitrate (60 wt.% $NaNO_3$ and 40 wt.% $KNO_3$), known as 'solar salt'. Both $NaNO_3$ and $KNO_3$ are commercialized by SQM® and have a purity of 98% and 99.3%, respectively. The main properties of such materials are presented in Table 1.

Table 1. Properties of the solar salt used (Kearney et al. 2003).

| **Property** | **Value** |
|---|---|
| Composition, wt.% | |
| $NaNO_3$ | 60 |
| $KNO_3$ | 40 |
| Freezing point, °C | 220 |
| Density @ 300 °C, kg/m$^3$ | 1899 |
| Dynamic viscosity @ 300 °C, kg/m·s | 3.26 $10^{-3}$ |
| Heat capacity @ 300 °C, J/kg K | 1495 |

## 2.2. Experimental set-up

### 2.2.1. Pilot plant description

The experimentation was carried out at the experimental facility designed and built at the University of Lleida with the purpose of simulating the operation of the TES system of a solar power plant at a lower scale (Fig. 2). Therefore, the design is as similar as possible to real facilities regarding materials, dimensions, etc., and it is integrated by a primary and a secondary circuits. The primary circuit consists on a two-tanks storage system where the molten salt charging and discharging process take place. The secondary circuit consists on: (a) a 24 $kW_e$ electrical heater which heats up Therminol-VP1 as heat transfer fluid (HTF), simulating the

solar collector field; (b) a 20 $kW_{th}$ air-HTF heat exchanger which cools the HTF down simulating the cooling technology to discharge the energy stored. The heat exchange between both molten salts and Tehrminol-VP1 fluids takes place in a plates heat exchanger (76H ALFANOVA supplied by Alfa-Laval). Measuring equipment to control, register and measure relevant variables such as flow, pressure and temperature has been integrated in the facility.

### 2.2.2. Storage system description

The two-tanks storage system consists of two identical tanks designed and built by GREA (Universitat de Lleida, Spain). The tanks design consists on a cylinder-shaped vessel closed with a flat circular plate at the bottom and a Klöpper cover on top, where the storage material is housed. All the elements of the tanks are made of stainless steel 316 L in order to withstand the elevate temperatures, to avoid galvanic corrosion, as well as to avoid compatibility problems between the storage material and the tank itself (Goods and Bradshaw, 2004). The cover of the vessel is manufactured with some openings in order to place the measuring devices and the molten salts pump. Table 2 shows the main geometrical characteristics of the tanks as well as some of the geometric characteristics of a commercial plant (Andasol-1 [16]. Notice that the pilot plant at the University of Lleida was designed with an aspect ratio (height per diameter ratio) as similar as possible to the commercial plants.

Table 2. Main geometrical characteristics of the storage tanks at the pilot plant and at a commercial plant

| | | **Pilot plant at the University of Lleida** | **Andasol-1 [16]** |
|---|---|---|---|
| **Parameter** | **Units** | **Value** | |
| Material | Stainless steel 316L | | - |
| Internal Diameter | [m] | 1.20 | 35.99 |
| Cylinder height | [m] | 0.50 | 14.00 |
| Aspect ratio | [-] | 0.41 | 0.39 |
| Klöpper cover height | [mm] | 267 | - |
| Total height | [mm] | 767 | - |
| Thickness of the walls | [mm] | 4 | - |

To minimize heat losses, 0.24 m of rock wool (Spintex 342G from Isover) is located around the walls and cover of the vessels. Moreover, 0.20 m of refractory concrete (Hormirefra) and 0.45 m of Foamglass ONE® are located under the tanks. Foamglass ONE® was selected because of its high compressive strength and mechanical stability at temperatures up to 481 ºC, quite higher than the maximum working temperature in the tank. The conductivity and thickness of these materials is specified in Table 3 and it is based on manufacturer data.

Table 3. Conductivity and thickness of the insulation materials, based on manufacturer data.

| **Insulation material (Manufacturer)** | **Conductivity [W/m·K]** | **Thickness [m]** |
|---|---|---|
| Spintex 342G (Isover) | $k_{Rock.wool}(T)$ = 0.0002·T+0.0252 | 0.24 |
| Refractory concrete (Hormirefra) | $k_{concrete}(T)$=0.0001·T+0.16 | 0.20 |
| Foamglass ONE® (Foamglass) | $k_{FoamGlass}(T)$ 0.0002·T+0.0364 | 0.45 |

In order to analyse temperature distribution within the tank, 27 calibrated temperature sensors (PT-100) with an accuracy of ±0.1 ºC were installed in each tank in contact with salts, distributed in three levels (at 10, 250 and 450 mm from the bottom of the tank) and in three branches separated 120 ºC, as Fig. 3 shows. These temperature sensors are located inside a stainless steel sheath in order to be protected from the molten salts corrosion.

Notice that for this study, only one tank is considered. This vessel incorporates four electrical resistances of 1 $kW_e$. Three of them have a metal sheath while one of them is in direct contact with the solar salts. The resistances are located at 110 – 114.3 mm (depending on the configuration) from the bottom of the tank and separated 90º each other in order to heat the molten salts up, similarly to those used in commercial solar power plants.

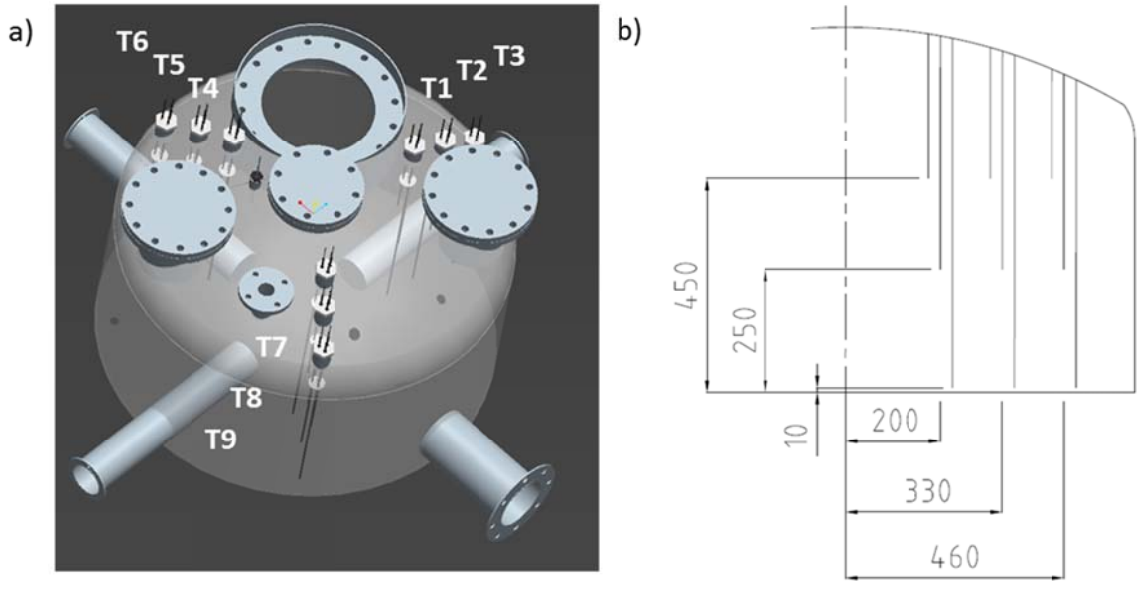


Fig. 3. Distribution of the temperature sensors in the storage tank (a) radial distribution of the groups of temperature sensors and (b) temperature sensors heights. Measures in mm.

In order to evaluate heat losses to the environment five surface temperature sensors (PT-100) have been used and placed in the transition of different insulating materials: between the external wall of the storage tank and the rock wool ($T_{Wall.in}$), on the external surface of the rock wool ($T_{Wall.ext}$), between the storage tank and the refractory concrete ($T_{Bottom}$), between the refractory concrete and the foam glass ($T_{Bottom.FG}$) and between the foam glass and the ground ($T_{Ground}$), as it can be seen in Fig. 4.

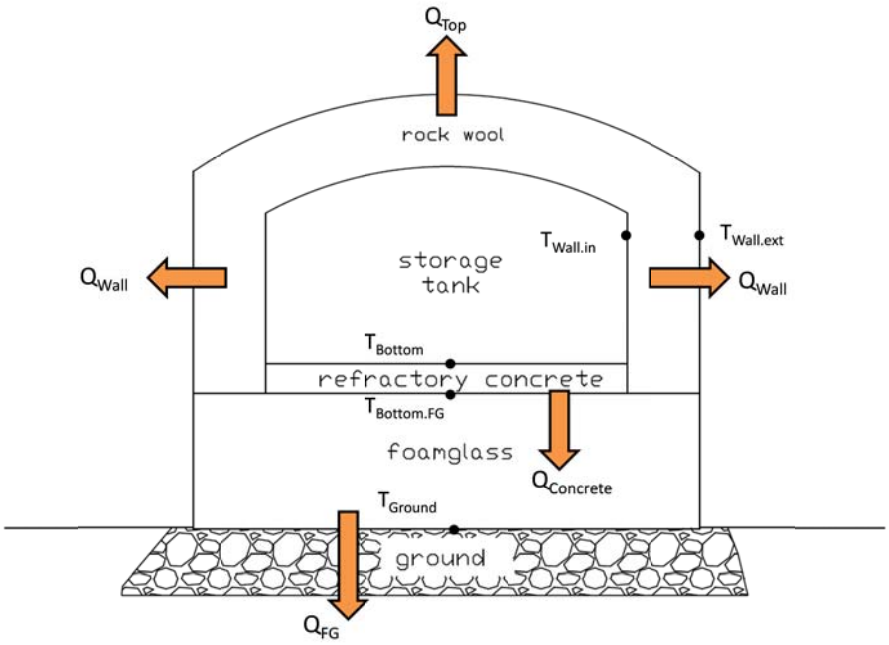


Fig. 4. Scheme of heat losses and temperature sensors used in the calculations

This experimentation was done with the storage tank fulfil with molten salts. In particular there are 966 kg of molten salts and they take up 50 cm.

## 2.3. Methodology

Both the temperature distribution test and the heat losses are evaluated by heating the salts up and, once the temperatures are homogenous, switching off the electrical resistances in the tank and recording the temperatures at different heights and location of the tank while cooling. This analysis takes into account the temporal evolution of the temperatures during the cooling process.

### 2.3.1. Temperature distribution tests

Before starting the temperature distribution tests, salts are heated up using the electrical resistances (in Fig. 5, energy consumption profile at 100%) until they reach a homogenous behaviour (steady state) needed approximately 120 hours. Then, the electrical resistances are

switched off (in Fig. 5, energy consumption profile at 0%) and the temperatures inside the tank start decreasing. At this moment, the temperature distribution test starts and it is named transient state. The tests consist on recording the temperatures in different heights and positions of the tank (Fig. 3) while molten salts maintain their liquid phase, from 400 to 290 ºC, approximately. Moreover, the temperature is recorded at three instants of time along the test: at the beginning, at the half and at the end of the temperature distribution test (see numbers 1, 2 and 3 from Fig. 5). Notice that salts are neither pumped nor moved inside the tank.

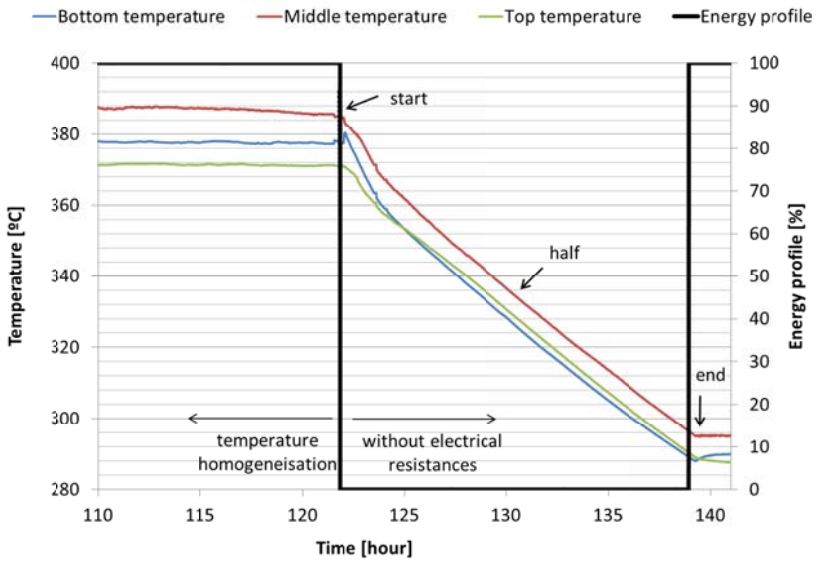


Fig. 5. Average storage tank temperatures by level and energy consumption profile. Start, half and end instants will be discussed in the article.

### 2.3.2. Heat losses

The heat losses from the tank per surface unit were calculated considering the conduction heat losses of the external wall surfaces of the tank ($Q_{Wall}$ and $Q_{Top}$), and the conduction heat losses at the bottom of the tank. On one hand, $Q_{Wall}$ is considered as both the heat losses of the walls and $Q_{Top}$ the heat losses of the cover of the vessel. On the other hand, the heat losses of the bottom of the tank are considered both heat losses through the refractory concrete ($Q_{Bottom}$) (Fig. 4).

To perform this study it had been necessary consider the assumptions below:

1. The temperature sensors located in the different surfaces of the tank are assumed to be representative for all the area that they represent (Fig. 4):
2. The insulation have low mass due to the low thickness the low density of the insulation. Therefore, in transient state it is considered that the insulation do not accumulate nor release energy.

3. The tank has been geometrically considered as a perfect cylinder with a bottom base and a sphere in the top (with surface correction factors shown in Eq. 3). Metal sheath containing electrical resistances have not been considered.
4. The whole system is considered in steady state. In this case the conduction heat losses should be the same as the convection and radiation ones and have not been considered. Conduction heat losses all along the experiment are also plotted.
5. The heat flow is considered unidirectional and normal to every exchange surface. Thus, the effect of the heat transfer along every material on the thermal behaviour of the tank is considered negligible.

Heat losses are quantified both during the homogenization of the temperatures and during the period without external salts heating (Fig. 5).

Then, heat losses from the tank walls to the ambient are calculated as shown in Eq. 1:

$$Q_{Wall} = \frac{k_{Rockwool} \cdot A_{Cyl}}{r} \cdot \frac{\left(T_{Wall.in} - T_{Wall.ext}\right)}{\ln\left(\frac{r_2}{r_1}\right)} \qquad \text{Eq. 1}$$

Heat losses from the Klöppler cover to the ambient are calculated as shown in Eq. 2:

$$Q_{Top} = \frac{0.1478}{r_1^{\,2}} \cdot \frac{k_{Rock.wool} \cdot A_{Sphere}}{r^2} \cdot \frac{\left(T_{Wall.in} - T_{Wall.ext}\right)}{\frac{r_2 - r_1}{r_1 \cdot r_2}} \qquad \text{Eq. 2}$$

Heat losses in the concrete are calculated as shown in Eq. 3:

$$Q_{Concrete} = k_{concrete} \cdot A_{concrete} \cdot \frac{\left(T_{Bottom} - T_{Bottom.FG}\right)}{\Delta_{x\,concrete}} \qquad \text{Eq. 3}$$

Moreover, how the heat losses vary depending on the scale of the facility is discussed comparing the pilot plant of the University of Lleida with higher scale commercial plants.

# 3. Results

## 3.1. Temperature distribution tests

The temperature distribution test lasts 17.13 hours which represents the time after the homogenization of the salts and until they are about to reach solidification temperature (transient state). The temperatures are evaluated in three dimensional sets: by level, by branch and by radial distance to the centre. The temperature profiles recorded in the three different

levels of the storage tank (bottom, middle and top) are analysed (Fig. 6). In general, it can be seen that the higher temperatures are found in the middle height temperature sensors. This may be due to the heat losses through the ground (section 3.4) and because the tank is not completely filled and the upper part is in contact with air. In general, it has been observed that values recorded in one of the branches (at T1, T2 and T3) positions are always slightly higher than the rest. This may be due to the proximity to the direct contact electric resistance.

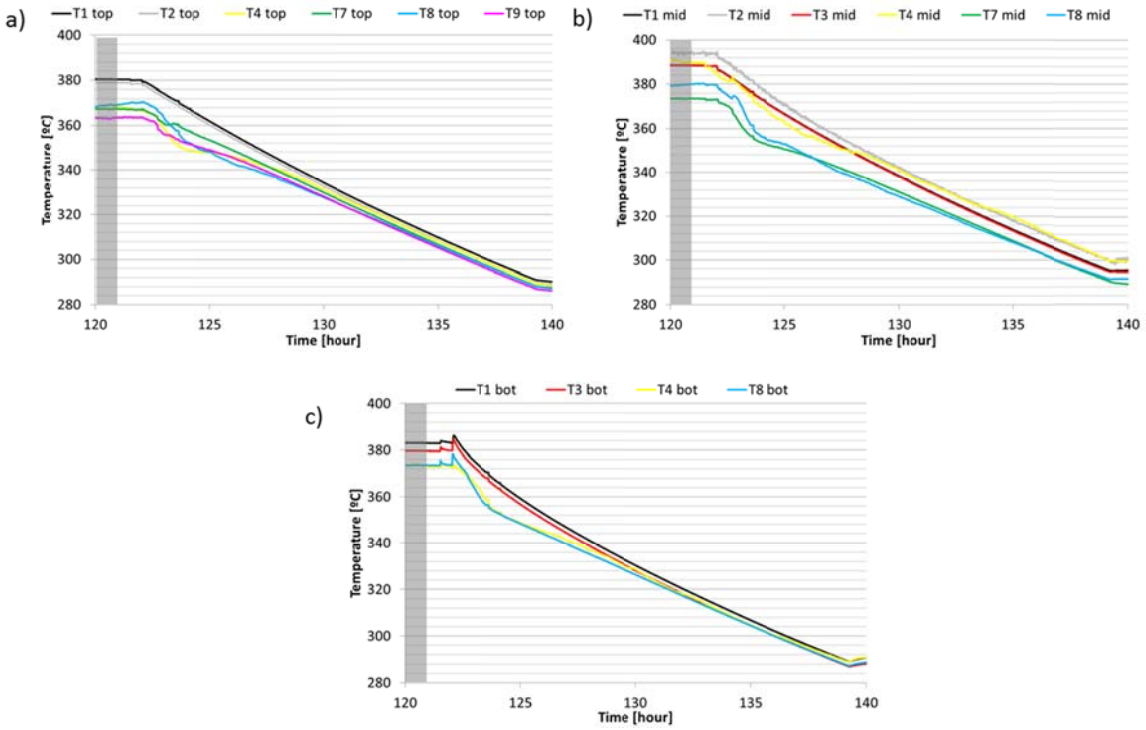


Fig. 6. General temperature profile by level: (a) bottom level; (b) middle level; (c) top level of salts, in grey: end of the steady state.

Regarding at the evaluation of the temperatures by level, Fig. 7 shows an overview of the temperatures of the whole tank at three different moments (at the start, at the half and at the end of the experimentation, see Fig. 5). It can be seen that the upper and bottom temperature levels (represented by a square) are more homogeneous than the middle level ones (represented by a circle). Moreover, as the time draws on, less temperature variation within the levels are obtained (a reduction from 40 to 60% of the temperature variation). As expected, no stratification is observed in the tank during this test.

Regarding at the evaluation of the temperatures by branch, the temperature distribution of sensors is compared in Fig. 8. The three branches are composed by the group of temperature sensors 1 to 3, 4 to 6 and 7 to 9 (Fig. 3). As expected, a temperature decrease through the time is observed. Notice however that the branch composed by the group of temperature sensors 7 to 9

is the one with colder values. This may be due to the facility layout: this branch is the most unprotected and expected to have more heat losses to the surroundings and more influence of the ambient temperature changes. This effect was previously observed by Prieto et al. (2015) in a similar facility, the Abengoa 8 $MW_{th}$ molten salts pilot plant located in Seville (Spain) and by Pachecho et al. (2002) in the Solar Two facility.

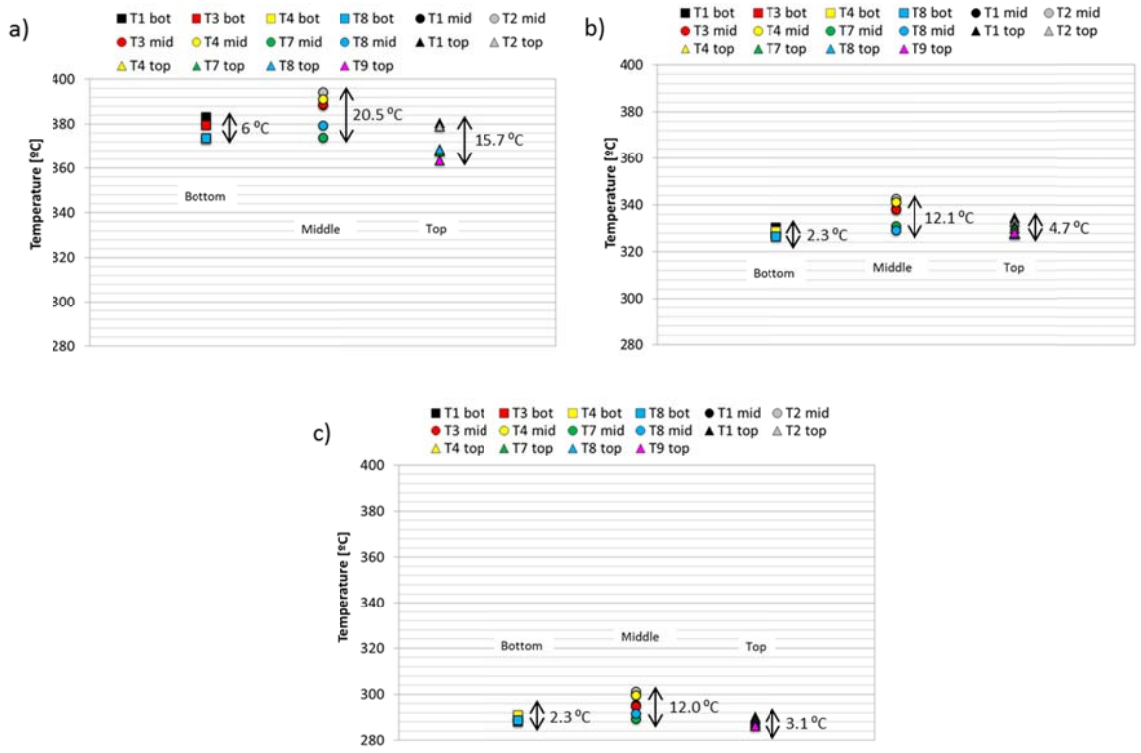


Fig. 7. Temperatures in the three levels of the tank at different times of the temperature distribution test: (a) start; (b) half; and (c) end.

Regarding at the evaluation of the temperatures by radial distance to the center (Fig. 9), the first group of temperature sensors is composed by T1, T4 and T7 (closest to the center of the tank), the second one by T2, T5 and T8 (middle), and the last one by T3, T6 and T9 (most external part of the tank). It can be seen that in the most external part of the tank, the temperatures tend to be less homogenous and lower than the rest.

After the evaluation of the temperatures, it can be seen that the main influencing parameters in the distribution temperature tests are: correct insulation of the tank, the existence of different electrical resistances (direct contact and with sheath) and the orientation and surroundings of the tank.

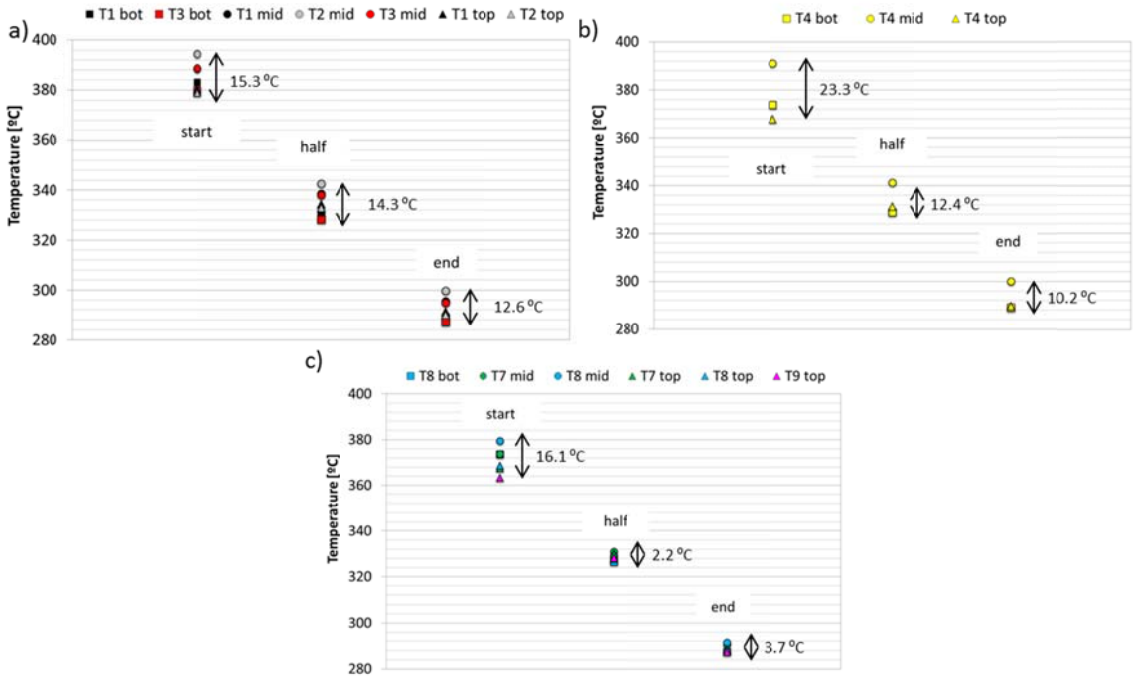


Fig. 8. Temperature distribution at the start, half and end of the temperature distribution test in the three different branches (a) branches 1 to 3, (b) branches 4 to 6 and (c) branches 7 to 9.

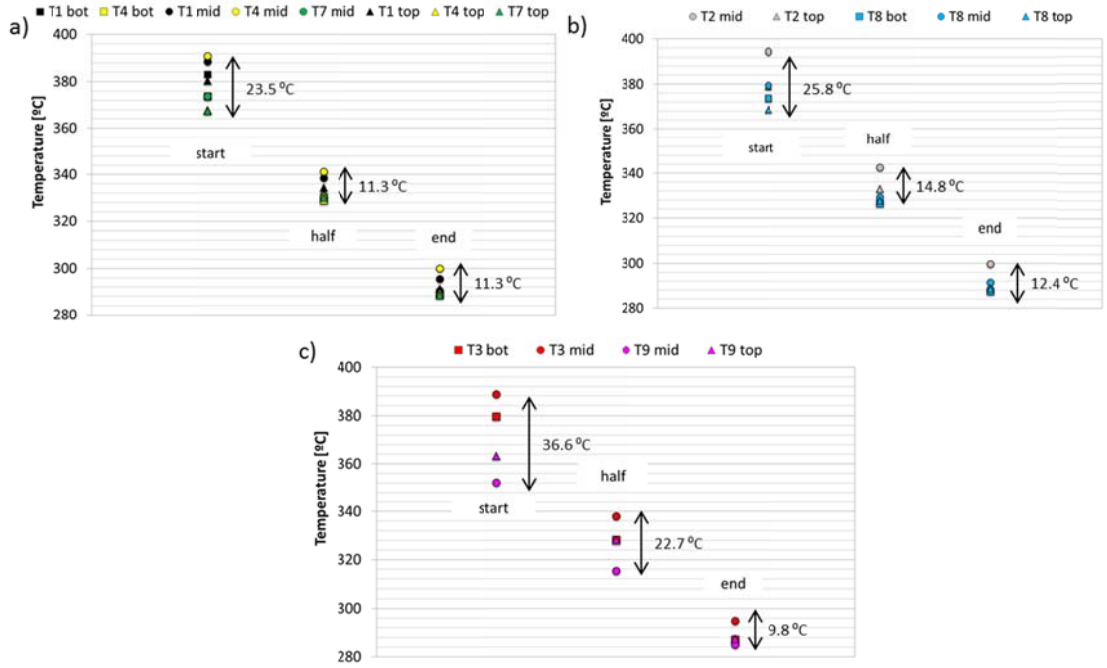


Fig. 9.Temperature distribution at the start, half and end of the experimentation in radial position: (a) closest to the center of the tank; (b) middle; and (c) most external part of the tank.

## 3.2. Heat losses

The temperature recorded by the surface sensors in the different parts of the tank as well as the energy profile of the electrical resistance are shown in Fig. 10 in order to show the temperature increases or decreases when the electrical heaters are switched on or off, respectively. This time-line corresponds to both the homogenization (steady state) period and the period without electrical heaters. The change from one period to the other is clearly shown in the sensors $T_{Wall.in}$ and in $T_{Bottom}$. The rest of the temperature sensors are slightly affected by the heat losses and remain almost constant throughout the experimentation time.

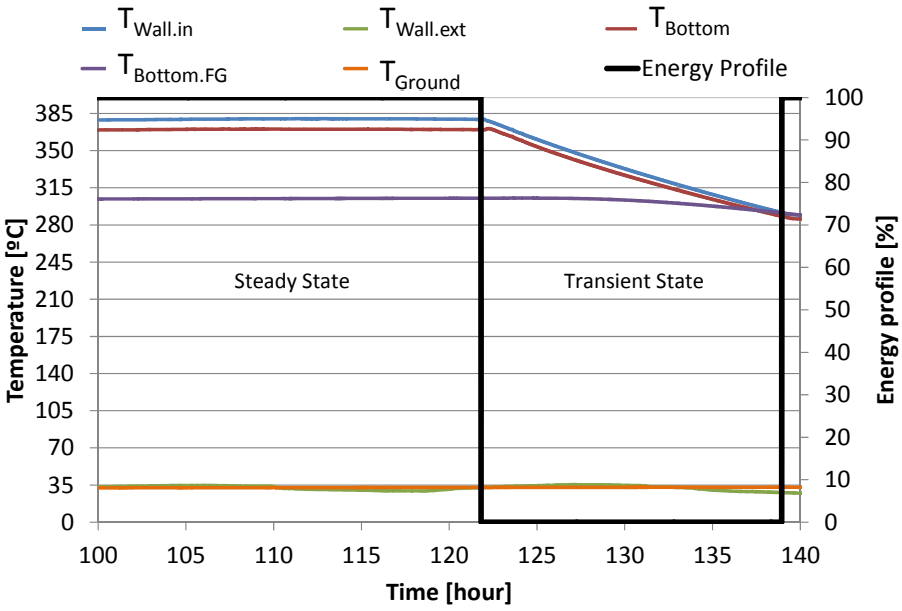


Fig. 10. Walls and bottom temperatures of the tank.

Moreover, in order to validate the experimental heat losses in the steady state part, a 1-D mathematical EES model has been performed. Constant thermophysical properties (conductivity, specific heat and density), homogeneous temperature in the tank (380 ºC), ambient temperature, and maximum level of salts (50 cm) have been assumed.

Table 2 summarizes results from the experiment, from the EES model and from a correlation published by Herrmann et al. 2004. These authors obtained this correlation from the Solar Two molten salts facility (Eq. 4) which is also composed of a two-tank TES facility configuration similar to the one in the pilot plant at the University of Lleida.

$$q_{loss} = 0.00017 \cdot T_{salt} + 0.012 \qquad \text{Eq. 4}$$

Table 4 shows that the top and wall experimental results have a good agreement with the data obtained in the EES model and the correlation found in the literature. The small differences seen can be due to the assumptions made in the model or to differences in insulation in the real plants. In the case of the bottom losses, the complexity of the model because of the refractory concrete and the lack of literature make impossible the comparison.

Table 4. Comparison of heat losses values, in W/m$^2$

| | **Experimental data** | **EES model** | **According to Herrmann et al. 2004** |
|---|---|---|---|
| Top | 72.70 | 72.25 | - |
| Walls | 79.13 | 79.60 | 76.00 |
| Bottom | 61.00 | - | - |

Regarding to the temperature evolution in the transient state, it can be seen that the temperature decrease is proportional to the distance to the heated part of the tank. Therefore the temperature sensors which show the most pronounced decrease are $T_{Wall.in}$, and $T_{bottom}$. Due to the thermal inertia of the refractory concrete, heat losses through the Foamglass® show a slightly decrease.

In order to discuss the effect of the scale in the heat losses, three different plants are compared: Solar Two, Andasol-1 and the pilot plant at the University of Lleida. For that an energy balance in transient state of a tank is presented (Eq. 5 and Eq. 6).

$$\frac{dQ}{dt} = \rho \cdot V \cdot Cp \cdot \frac{dT}{dt} \qquad \text{Eq. 5}$$

$$\frac{dQ}{dt} = h \cdot A_{cyl} \cdot \Delta T \qquad \text{Eq. 6}$$

Assuming that all the heat losses to the surroundings are in form of convection and that ΔT, h, cp and ρ are the same for the different plants considered; it is observed that heat losses are proportional to the shape factor (which is the surface are to volume ratio) of the storage tank (Eq. 7).

$$\frac{dT}{dt} = \frac{h \cdot A_{cyl} \cdot \Delta T}{\rho \cdot V \cdot Cp} = \frac{A_{cyl}}{V} \cdot cnt \qquad \text{Eq. 7}$$

The geometric characteristic of these three different scale TES tanks are listed in Table 5 The shape factor of the three plants belong to, in descending order, to the pilot plant of the University of Lleida, the Solar Two plant and Andasol-1 plant. So, the heat losses are expected to be higher in the pilot plant of the University of Lleida.

Table 5. Geometric characteristics of three different scales of TES systems for solar power plants

| | | **Pilot plant University of Lleida** | **Solar Two [14]** | **Andasol-1 [16]** |
|---|---|---|---|---|
| **Parameter** | **Units** | **Value** | | |
| Surface | [$m^2$] | 1.90 | 306.12 | 1583.36 |
| Volume | [$m^3$] | 0.57 | 769.51 | 18904.42 |
| Shape factor | [$m^{-1}$] | 3.33 | 0.40 | 0.08 |

# 4. Conclusions

Two-tank storage system with molten salts used commercially in solar power plants is evaluated experimentally through temperature distribution inside the tanks and heat losses analysis at pilot plant scale. This pilot plant was designed and built at the University of Lleida (Spain).The advantages of using this facility is, first, that it has a design very similar to real commercial facilities and, second, that the facility is equipped with many temperature sensors and other measurement equipment which makes possible an exhaustive study of the processes and which has not been found in the literature yet.

The thermal behaviour of a tank of salt will be very conditioned by two factors; the thermal losses through walls or foundations and thermal distribution inside the tank that occurs due to these losses. Therefore, this pilot plant is provided of several temperature sensors both inside the tank and in the different layers of external insulation.

On one hand, temperature distribution evolution is measured in transient state conditions, once the electrical resistances are switched off after a temperature stabilization period. The temperature distribution is evaluated in the different levels measured it may be seen that losses through the bottom by conduction and losses through the top (because of direct contact with air) are higher than in the middle of the tank. When the orientation of the tank is taken into consideration (by comparing the different branches of instrumentation), it can be seen that the more unprotected part has lower temperatures. It has been observed that the influencing parameters in the distribution temperature in the tank are: suitable and uniform insulation of the tank and the existence of different electrical resistances (direct contact and with sheath).

On the other hand, experimental heat losses have been calculated in steady state conditions (with the electrical resistances switched on) and then compared to those simulated with a 1-D model and to those obtained with a correlation published previously in the literature in a similar facility. Calculated heat losses were of about 80 W/$m^2$ through the walls, 73 W/$m^2$ through the cover, and 61 W/$m^2$ through the concrete located at the bottom of the tank. The calculated

values agree with the simulation and the correlation. As expected, the heat losses through the walls, cover and concrete decrease when the heating system of the tank is stopped, but those through the foam glass remain nearly constant.

## Acknowledgements

Special thanks to Jaume Gasia from University of Lleida (Spain). The research leading to these results has received funding from Spanish goverment (Fondo tecnológico IDI-20090393, ConSOLida CENIT 2008-1005) and from Abengoa Solar NT. The work is partially funded by the Spanish government (ENE2008-06687-C02-01/CON, ENE2011-22722, ENE2015-64117-C5-1-R, and ULLE10-4E-1305). The authors would like to thank the Catalan Government for the quality accreditation given to their research group GREA (2014 SGR 123). This project has received funding from the European Commission Seventh Framework Programme (FP/2007-2013) under Grant agreement Nº PIRSES-GA-2013-610692 (INNOSTORAGE) and from the European Union's Horizon 2020 research and innovation programme under grant agreement No 657466 (INPATH-TES). Laia Miró would like to thank the Spanish Government for her research fellowship (BES-2012-051861).

## References

1. Blake, D., Price, H., 2003. Assessment of a molten salt heat transfer fluid in a parabolic trough solar field. ASME J. Sol. Energy Eng. 125,170-176.
2. Collado, F.J., Guallar, J., 2013. A review of optimized design layouts for solar power tower plants with campo code. Renew. Sust. Energ. Rev 20, 142-154.
3. Foamglas http://www.foamglas.es/es/productos/descripcin/paneles_foamglas/
4. Gabrielli, R., Zamparelli C., 2009. Optimal Design of a Molten Salt Thermal Storage Tank for Parabolic Trough Solar Power Plants. ASME J. Sol. Energ. Eng. 131, 041001.
5. Gil, A., Medrano, M., Martorell, I., Lázaro, A., Dolado, P., Zalba, B., Cabeza, L.F., 2010. State of the art on high temperature thermal energy storage for power generation. Part 1—Concepts, materials and modellization. Renew. Sust. Energ. Rev. 14, 31–55.
6. Goods, S.H., Bradshaw, R.W., 2004. Corrosion of Stainless Steels and Carbon Steel by Molten Mixtures of Commercial Nitrate Salts. J. Mater. Eng. Perform. 13:78-87.
7. Herrmann, U., Kelly, B., Price, H., 2004. Two-tank molten salt storage for parabolic trough solar power plants. Energy 29, 883-893.
8. Hormirefra http://www.hormirefra.es/catalogos/horlite/HORLITE%20124%20B.pdf
9. International Energy Agency. Technology Roadmap: Solar Thermal Electricity.2014.
10. Isover http://www.isover.es/Media/Files/Productos-AT/Declaraciones-CE/MANTA-SPINTEX-342-G

11. Kearney, D., Herrmann, U., Nava, P., Kelly, B., Mahoney, R., Pacheco, J., Cable, R., Potrovitza, N., Blake, D., Price, H., 2003. Assessment of a molten salt heat transfer fluid in a parabolic trough solar field. ASME J. Sol. Energ. Eng. 125, 170-176.
12. Medrano, M., Gil, A., Martorell, I., Potau, X., Cabeza, L.F., 2010. State of the art on high-temperature thermal energy storage for power generation. Part 2—Case studies. Renew. Sust. Energ. Rev. 14, 56–72.
13. Moens, L., Blake, D.M., Rudnicki, D.L., Hale, M.J., 2003. Advanced Thermal Storage Fluids for Solar Parabolic Trough Systems. ASME J. Sol. Energ. Eng. 125, 112–116.
14. Pacheco, J.E., 2002. Final test and evaluation results from the Solar Two project. 2002.
15. Prieto, C., Fernández, A.I., Cabeza, L.F. Molten salt facilities, lessons learnt at pilot plant scale to guarantee commercial plants. Part 1 – Plant description and start-up recommendations. Submitted to Applied Energy 2015.
16. Solar Millenium AG. The parabolic trough power plants Andasol 1 to 3. https://www.rwe.com/web/cms/mediablob/en/1115150/data/0/1/Further-information-about-Andasol.pdf
17. Suarez, C., Iranzo, A., Pino, F.J., Guerra, J., 2015. Transient analysis of the cooling process of molten salt thermal storage tanks due to standby heat loss. Appl. Energ. 142, 56-65.
18. Zaversky, F., García-Barberena, J., Sánchez, M., Astrain, D., 2013. Transient molten salt two-tank thermal storage modelling for CSP performance simulations. Sol. Energ. 93, 294-311.